J Supercond Nov Magn (2009) 22: 205–208
DOI 10.1007/s10948-008-0377-1

ORIGINAL PAPER

Phase Transition and Anomalous Low Temperature Ferromagnetic Phase in $Pr_{0.6}Sr_{0.4}MnO_3$ Single Crystals

S. Rößler · S. Harikrishnan · C.M. Naveen Kumar · H.L. Bhat · Suja Elizabeth · U.K. Rößler · F. Steglich · S. Wirth

Received: 16 October 2008 / Accepted: 20 October 2008 / Published online: 30 October 2008

Abstract We report on the magnetic and electrical properties of $Pr_{0.6}Sr_{0.4}MnO_3$ single crystals. This compound undergoes a continuous paramagnetic-ferromagnetic transition with a Curie temperature $T_C \sim 301$ K and a first-order structural transition at $T_S \sim 64$ K. At T_S, the magnetic susceptibility exhibits an abrupt jump, and a corresponding small hump is seen in the resistivity. The critical behavior of the static magnetization and the temperature dependence of the resistivity are consistent with the behavior expected for a nearly isotropic ferromagnet with short-range exchange belonging to the Heisenberg universality class. The magnetization (M–H) curves below T_S are anomalous in that the virgin curve lies outside the subsequent M–H loops. The hysteretic structural transition at T_S as well as the irreversible magnetization processes below T_S can be explained by phase separation between a high-temperature orthorhombic and a low-temperature monoclinic ferromagnetic phase.

Keywords Manganites · Phase separation

1 Introduction

Perovskite oxides of the type $R_{1-x}A_xMnO_3$ (R = rare earth ion, A = divalent ion) exhibit remarkable physical properties including colossal magnetoresistance, charge/orbital order and a complex magnetic phase diagram. Extensive studies on these materials revealed that the physical properties are very sensitive to subtle structural distortions. One peculiar case is the $Pr_{1-x}Sr_xMnO_3$ system. The parent compound $PrMnO_3$ crystallizes in an orthorhombic structure and is an A-type antiferromagnetic (AFM) insulator. Doping of Sr^{2+} ions leads to a ferromagnetic (FM) metallic phase for $0.2 < x < 0.4$ [1]. Various AFM structures result for higher strontium doping [2, 3]. A first-order transition from a FM metallic to an AFM insulating phase has been observed in $Pr_{0.5}Sr_{0.5}MnO_3$ [4]. This kind of transition persists only up to $x = 0.55$ [5]; compounds with higher doping level x remain insulating. Initially, this first-order transition was interpreted as a charge-ordered state with a CE-type AFM phase below 135 K, later it was confirmed that the AFM order is of A-type [6]. However, from neutron diffraction studies on $Pr_{0.5}Sr_{0.5}MnO_3$ a different type of stripe-like charge order with wave vector $\boldsymbol{q} \sim (0, 0, 0.3)$ at all temperatures was inferred [7]. The FM–AFM phase transition is also associated with a structural transition from the tetragonal to monoclinic phase [8]. The metallic FM phase can be restored by application of a magnetic field of about 7 T [4]. In contrast, at somewhat lower doping a different structural transition was observed: In $Pr_{0.6}Sr_{0.4}MnO_3$ a transition from an orthorhombic (space group *Pnma*) to a monoclinic (space group $I2/a$) structure was inferred from powder neutron diffraction [9]. This phase transition is incomplete: even at 1.6 K a 12% volume fraction of the high-temperature orthorhombic phase persists [9]. However, unlike the half-doped $x = 0.5$ compound, $Pr_{0.6}Sr_{0.4}MnO_3$ remains FM and metallic down to lowest temperature. ^{55}Mn nuclear magnetic resonance (NMR) measurements showed a single resonance peak at a frequency corresponding to an average value of the Mn^{4+} and Mn^{3+} resonance frequencies. This result rules out the

S. Rößler · F. Steglich · S. Wirth (✉)
Max Planck Institute for Chemical Physics of Solids, Nöthnizer Straße 40, 01187 Dresden, Germany
e-mail: wirth@cpfs.mpg.de

S. Harikrishnan · C.M. Naveen Kumar · H.L. Bhat · S. Elizabeth
Department of Physics, Indian Institute of Science, C.V. Raman Avenue, Bangalore 560012, India

U.K. Rößler
IFW Dresden, Postfach 270016, 01171 Dresden, Germany

possibility of short-range charge order and confirms a homogeneous metallic state [10]. Here, we investigate the nature of the FM transition in $Pr_{0.6}Sr_{0.4}MnO_3$ single crystals by measuring a series of magnetization isotherms encompassing the Curie temperature T_C. We also show that the temperature derivative of the resistivity displays a critical behavior. Further, we illustrate that at temperatures below the structural transition, i.e. $T < T_S$, the magnetization processes are anomalous with a strong dependence on the magnetic history resulting from a phase separation between the orthorhombic and the monoclinic FM phases.

2 Experimental

Single crystals of $Pr_{0.6}Sr_{0.4}MnO_3$ were grown by the floating-zone method. The crystals were characterized by Laue back scattering, powder x-ray diffraction (XRD) and transmission electron microscopy. The composition was confirmed by inductively coupled plasma emission spectroscopy (ICPES). The resistivity and ac-susceptibility were obtained using a physical property measurement system (PPMS by Quantum Design) and isothermal magnetization measurements were conducted in a superconducting quantum interference device magnetometer (MPMS by Quantum Design).

3 Results and Discussion

The temperature dependence of the ac-susceptibility, $\chi'(T)$, measured along the crystallographic a axis with a frequency of 1333 Hz and an amplitude of 10 Oe is presented in Fig. 1. A clear FM transition is observed around 300 K. In addition, $\chi'(T)$ displays an abrupt jump at around 64 K (notated as T_S) in the cooling cycle. This transition exhibits a sizeable thermal hysteresis in $\chi'(T)$ as it is shifted by about 10 K (towards higher T) in the warming cycle. These data suggest that this transition is of first order. The decrease of $\chi'(T)$ at T_S when lowering the temperature indicates that the easy axis of magnetization turns away from the c axis. A similar jump in magnetization has been reported in polycrystalline $Pr_{0.6}Sr_{0.4}MnO_3$ [11]. Hence, we attribute this jump to the structural transition also observed in neutron diffraction studies [9]. In contrast, the FM transition at T_C appears to be continuous and to take place in a homogeneous structural state.

Figure 2 depicts the temperature dependence of the resistivity, $\rho(T)$, indicating metallic behavior from 400 K down to 5 K. The two anomalies are clearly resolved in $\rho(T)$: (i) at T_C the resistivity drops abruptly and (ii) at T_S a hump in the resistivity is observed. In the temperature range 130–240 K, the resistivity follows a T^2 dependence (inset of Fig. 2) indicating that $Pr_{0.6}Sr_{0.4}MnO_3$ is in a Fermi liquid state. The temperature dependence of the resistivity above T_C is similar to the one observed for $La_{0.7}Sr_{0.3}MnO_3$ which transforms from an incoherent metal to a coherent one at T_C [12]. The sharp drop in $\rho(T)$ at T_C results from the reduced contribution of magnetic scattering. The temperature derivative of resistivity, $d\rho/dT$, shows a peak at T_C (Fig. 3). A similar behavior is also observed in $La_{0.7}Ca_{0.3}MnO_3$. In metallic ferromagnets, $d\rho/dT$ is expected to exhibit the same critical behavior as the specific heat following the Fisher–Langer relation [13]. Therefore, we attempted a critical fit to the re-

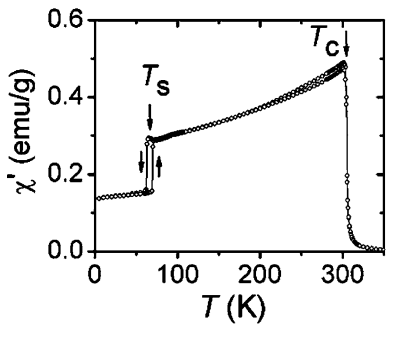

Fig. 1 ac-susceptibility as a function of temperature. The cooling and heating cycle exhibit a sizable thermal hysteresis around the structural transition T_S

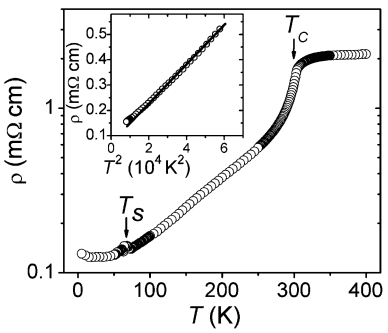

Fig. 2 The temperature dependence of resistivity $\rho(T)$ presented in a semi-logarithmic plot. In the inset, the experimental data $\rho(T)$ below T_C are compared to a T^2 law (*solid line*)

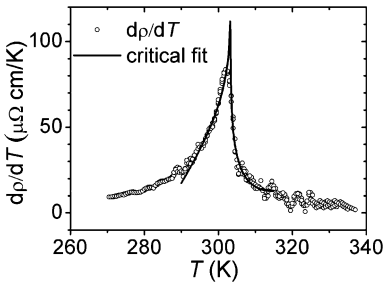

Fig. 3 $d\rho/dT$ in dependence on T showing the critical anomaly around T_C. The continuous line is the fit to the data as explained in the text

sistivity data with the standard expressions

$$\mathrm{d}\rho/\mathrm{d}T = \left(A^{+}\right)|\varepsilon|^{-\alpha} + B|\varepsilon| + C \quad \text{for } T < T_{\mathrm{C}} \tag{1}$$

and

$$\mathrm{d}\rho/\mathrm{d}T = \left(A^{-}\right)|\varepsilon|^{-\alpha} + B|\varepsilon| + C \quad \text{for } T > T_{\mathrm{C}}. \tag{2}$$

Here, A^{+}/A^{-} is the universal amplitude ratio, $\varepsilon = T - T_{\mathrm{C}}/T_{\mathrm{C}}$ the reduced temperature, α denotes the specific heat exponent and B the coefficient of the non-magnetic common linear background. Unfortunately, a fit to the data leaving all parameters free was inconclusive as parameters became strongly correlated. Therefore, both equations (1) and (2) were fitted simultaneously to the $\mathrm{d}\rho/\mathrm{d}T$ vs. T data by fixing the exponent to the expected value pertaining to the Heisenberg universality class $\alpha = -0.133$. The temperature range considered in the fitting procedure was $294\ \mathrm{K} \leq T \leq 313\ \mathrm{K}$, with the data in the rounded region of 300–303 K left off. The results of this fit are compared to the experimental data $\mathrm{d}\rho/\mathrm{d}T$ in Fig. 3. The fit yields the universal amplitude ratio $A^{+}/A^{-} = 1.49$ (± 0.02) and $T_{\mathrm{C}} = 303.29$ (± 0.01) K. This value of the amplitude ratio is close to the one expected for the 3D Heisenberg universality class ($A^{+}/A^{-} = 1.53$). Hence, our results are consistent with the expected behavior at the continuous transition of a nearly isotropic ferromagnet.

In order to further characterize the FM phase transition, we carried out a series of isothermal magnetization measurements around T_{C}. According to the mean-field theory for a continuous phase transition, the magnetization M close to T_{C}—when plotted as M^2 vs. H/M (Arrott plots)—should yield a series of straight lines, with the line at $T = T_{\mathrm{C}}$ passing through the origin [14]. In the present case, we found nonlinear Arrott plots indicating that the mean-field theory is not applicable. This is not surprising since $M(H, T)$ of a magnet belonging to the Heisenberg universality class is to be described by modified exponents $\beta = 0.38$ and $\gamma = 1.33$ in $M^{1/\beta}$ and $(H/M)^{1/\gamma}$ (from mean-field theory $\beta = 0.5$ and $\gamma = 1.0$ resulting in the Arrott plot). With these trial values for β and γ, so-called *modified* Arrott plots give rise to perfectly linear lines for all temperatures, Fig. 4. At $T = 301$ K, the line passes through the origin suggesting that $T_{\mathrm{C}} \approx 301$ K. Typically, for manganites the linear behavior in the modified Arrott plots is observed only for high applied fields [15]. The remarkably parallel and linear lines in Fig. 4 imply that an influence of competing AFM interactions is absent, and $Pr_{0.6}Sr_{0.4}MnO_3$ behaves similarly to typical metallic ferromagnets, like Fe or Ni. We note that the spontaneous magnetization and the inverse susceptibility can be obtained from such modified Arrott plots (a detailed analysis of the critical properties will be presented elsewhere [16]). Our analysis of the modified Arrott plots and the resistivity based on the Fisher–Langer relation suggests that the

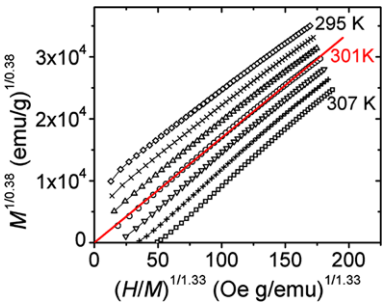

Fig. 4 The modified Arrott plots $M^{1/\beta}$ vs. $(H/M)^{1/\gamma}$ with the exponents $\beta = 0.38$ and $\gamma = 1.33$ at different measurement temperatures. T_{C} is obtained from the temperature at which the $M^{1/\beta}$ vs. $(H/M)^{1/\gamma}$ line extrapolates to the origin

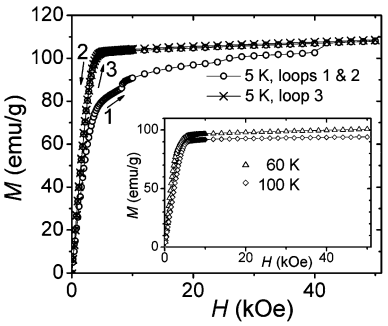

Fig. 5 M–H curves at 5 K after cooling the sample in zero field. The virgin curve (loop 1) lies outside the subsequent magnetization curves (loops 2 and 3). Inset: M–H curves at 60 and 100 K

critical properties of the paramagnetic–ferromagnetic transition in $Pr_{0.6}Sr_{0.4}MnO_3$ are close to those of a 3D Heisenberg ferromagnet with short-range interactions.

Below the structural transition, the magnetization processes are anomalous. In Fig. 5, the magnetization curves $M(H)$ at 5 K, 60 K and 100 K are shown. The measurements were carried out after cooling the sample in zero field. At 5 K, the virgin curve (loop 1) stays below all subsequent $M(H)$ loops (independently of sweep direction, loops 2 and 3) and displays a series of characteristic jumps at about 10, 28 and 40 kOe. Since hysteresis, remanence and coercive field of all these curves are vanishingly small, a prominent influence of the rare-earth (Pr) magnetism is unlikely. However, a phase separation of $Pr_{0.6}Sr_{0.4}MnO_3$ into a monoclinic FM and an orthorhombic phase at low temperature has been reported earlier [9]. The transformation process on cooling apparently remains incomplete in zero field, probably due to problems in accommodating the low-symmetry phase inside the orthorhombic high-temperature phase. Therefore, the observed magnetic properties are likely related to a field-driven structural phase transition. A similar magnetic behavior led to the inference of phase separation in Al-substituted $Pr_{0.5}Sr_{0.5}MnO_3$ but involves the more commonly observed FM metallic to AFM insulating phase transition [17]. We note that sev-

eral scenarios are possible to describe the effects depending on whether magnetic fields favor the monoclinic or the orthorhombic phase. As an example, a field-driven structural transition might occur if the two phases have different spontaneous magnetic moments. This might well be the case here since the spontaneous magnetic moment in these manganites strongly depends on the Mn–O–Mn bond-bending which differs in the two lattice structures. However, at present it is not known which of the two structures in the phase-separated microstructure of $Pr_{0.6}Sr_{0.4}MnO_3$ owns the higher spontaneous magnetization. Still, a transformation back from the monoclinic low-temperature phase to the orthorhombic high-temperature phase may be favored by the magnetic order in this compound, similarly to structural transformations in fields in certain magnetic Heusler alloys [18]. A shift of phase boundaries in a fine microstructure explains the high driving fields for the transformation process and the irreversible character of the magnetization process.

An alternative mechanism might favor a redistribution of crystallographic variants and structural phases due to different magnetocrystalline anisotropies. Such a mechanism would resemble the recently investigated behavior of ferromagnetic martensites, the so-called magnetic shape-memory materials [19]. However, the absence of strong hysteresis in the subsequent $M(H)$ curves (loops 2 and 3 in Fig. 5) *after* the transformation process likely rules out a strong magnetocrystalline anisotropy as source of the observed transition. We note that at temperatures very close to and above the structural transition (inset of Fig. 5) an anomalous magnetization behavior is not observed. Further investigations are needed to pinpoint the structural features and the irreversible and incomplete character of the transformation processes around T_S.

In conclusion, metallic $Pr_{0.6}Sr_{0.4}MnO_3$ displays conventional magnetic behavior around T_C that can be described within the 3D Heisenberg universality class. However, below a structural phase transition, complex magnetic behavior is observed that is likely caused by a heterogeneous, phase-separated state with different crystallographic and magnetic phase fractions coexisting. The distinctive feature of this manganite relies on the fact that these effects take place in a FM metallic system, as opposed to more conventional cases (such as half-doped manganites or $Pr_{1-x}Ca_xMnO_3$ [20]) in which an AFM phase and charge- or orbital-order compete with a FM metallic state.

Acknowledgement We thank the European Commission for financial support through CoMePhS 517039.

References

1. Knížek, K., Jirák, Z., Pollert, E., Zounová, F., Vratislav, S.: J. Solid State Chem. **100**, 292 (1992)
2. Kolensik, S., Dabrowski, B., Chmaissem, O., Bukowski, Z., Mais, J.: J. Appl. Phys. **89**, 7407 (2001)
3. Chmaissem, O., Dabrowski, B., Kolensik, S., Mais, J., Jorgensen, J.D., Short, S.: Phys. Rev. B **67**, 094431 (2003)
4. Tomioka, Y., Asamitsu, A., Moritomo, Y., Kuwahara, H., Tokura, Y.: Phys. Rev. Lett. **74**, 5108 (1995)
5. Hervieu, M., Martin, C., Maignan, A., van Tendeloo, G., Jirak, Z., Hejtmanek, J., Barnabé, A., Thopart, D., Raveau, B.: Chem. Mater. **12**, 1456 (2000)
6. Kawano, H., Kajimoto, R., Yoshizawa, H., Tomioka, Y., Kuwahara, H., Tokura, Y.: Phys. Rev. Lett. **78**, 4253 (1997)
7. Kajimoto, A., Yoshizava, H., Tomioka, Y., Tokura, Y.: Phys. Rev. B **66**, 180402(R) (2002)
8. Llobet, A., García-Munoz, J.L., Frontera, C., Ritter, C.: Phys. Rev. B **60**, 9889(R) (1999)
9. Ritter, C., Radaelli, P.G., Lees, M.R., Barratt, J., Balakrishnan, G., Paul, D.McK.: J. Solid State Chem. **127**, 276 (1996)
10. Boujelben, W., Ellouze, M., Cheikh-Rouhou, A., Pierre, J., Cai, Q., Yelon, W.B., Shimizu, K., Dubourdieu, C.: J. Alloys Compd. **334**, 1 (2002)
11. Boujelben, W., Cheikh-Rouhou, A., Ellouze, M., Joubert, J.C.: Phys. Stat. Sol. **177**, 503 (2000)
12. Urushibara, A., Moritomo, Y., Arima, T., Asamitsu, A., Kido, G., Tokura, Y.: Phys. Rev. B **51**, 14103 (1995)
13. Fisher, M.E., Langer, J.S.: Phys. Rev. Lett. **20**, 665 (1968)
14. Arrott, A., Noakes, J.E.: Phys. Rev. Lett. **19**, 786 (1967)
15. Sahana, M., Rößler, U.K., Ghosh, N., Elizabeth, S., Bhat, H.L., Dörr, K., Eckert, D., Wolf, M., Müller, K.-H.: Phys. Rev. B **68**, 144408 (2003)
16. Harikrishnan, S. et al.: unpublished
17. Banerjee, A., Kumar, K., Chaddah, P.: arXiv:0805.1514
18. Kainuma, R., Imano, Y., Ito, W., Sutou, Y., Morito, H., Okamoto, S., Kitakami, O., Oikawa, K., Fujita, A., Kanomata, T., Ishida, K.: Nature **439**, 957 (2006)
19. O'Handley, R.C.: J. Appl. Phys. **83**, 3263 (1998)
20. Tokura, Y.: Rep. Prog. Phys. **69**, 797 (2006)